OXFORD

Cerebral Cortex, 2023, **33**, 1895–??

https://doi.org/10.1093/cercor/bhac180

Advance access publication date 10 May 2022

Original Article

White matter microstructural variability linked to differential attentional skills and impulsive behavior in a pediatric population

Anthony Gagnon[1], Gabrielle Grenier[2], Christian Bocti[3,4], Virginie Gillet[1], Jean-François Lepage[1], Andrea A Baccarelli[5], Jonathan Posner[6], Maxime Descoteaux[2,7,†], Larissa Takser[1,8,†*]

[1]Department of Pediatrics, University of Sherbrooke, Sherbrooke, Quebec, Canada,
[2]Sherbrooke Connectivity Imaging Laboratory (SCIL), Université de Sherbrooke, Sherbrooke, Quebec, Canada,
[3]Department of Medicine, Université de Sherbrooke, Sherbrooke, Quebec, Canada,
[4]Research Center on Aging, CIUSSS de l'Estrie-CHUS, Sherbrooke, Quebec, Canada,
[5]Department of Environmental Health Sciences, Columbia University Mailman School of Public Health, New York, NY, USA,
[6]Department of Psychiatry, Duke University, Durham, NC, USA,
[7]Imeka Solutions Inc, Sherbrooke, QC, Canada,
[8]Department of Psychiatry, University of Sherbrooke, Sherbrooke, Québec, Canada,
*Corresponding author: Larissa Takser, MD, PhD, Département de Pédiatrie, Faculté de Médecine et des sciences de la santé, Université de Sherbrooke, 3001, 12ième Avenue Nord, Sherbrooke, QC, Canada J1H 5N4. Email: Larissa.Takser@USherbrooke.ca

†Maxime Descoteaux and Larissa Takser are co-senior authors. These authors contributed equally.

Structural and functional magnetic resonance imaging (MRI) studies have suggested a neuroanatomical basis that may underly attention-deficit–hyperactivity disorder (ADHD), but the anatomical ground truth remains unknown. In addition, the role of the white matter (WM) microstructure related to attention and impulsivity in a general pediatric population is still not well understood. Using a state-of-the-art structural connectivity pipeline based on the Brainnetome atlas extracting WM connections and its subsections, we applied dimensionality reduction techniques to obtain biologically interpretable WM measures. We selected the top 10 connections-of-interests (located in frontal, parietal, occipital, and basal ganglia regions) with robust anatomical and statistical criteria. We correlated WM measures with psychometric test metrics (Conner's Continuous Performance Test 3) in 171 children (27 Dx ADHD, 3Dx ASD, 9–13 years old) from the population-based GESTation and Environment cohort. We found that children with lower microstructural complexity and lower axonal density show a higher impulsive behavior on these connections. When segmenting each connection in subsections, we report WM alterations localized in one or both endpoints reflecting a specific localization of WM alterations along each connection. These results provide new insight in understanding the neurophysiology of attention and impulsivity in a general population.

Key words: diffusion MRI; white matter connectivity; cognitive functions; tractography; child & adolescent;

Introduction

Inhibition capabilities are essential in human development and are strong predictors of social and educational life outcomes (Mischel and Ebbesen 1970; Shoda et al. 1990). Although many other factors can impact one's ability to delay gratification, it remains an important contributor to attentional skills as well as impulsive behaviors (Bari and Robbins 2013). Over the years, inhibition capabilities have mostly been associated with the right inferior cortex, the pre-motor supplementary area and the subthalamic nucleus (Aron and Poldrack 2006; Aron et al. 2007). Functional magnetic resonance imaging (MRI) studies have reported numerous times the prefrontal cortex as the main activated regions during response inhibition in adults (Rubia et al. 2003; Aron and Poldrack 2006; Aron et al. 2007; Chevrier et al. 2007). The WM fascicles comprise in the right inferior frontal gyrus and pre-motor supplementary area have also been associated with response inhibition in a diffusion MRI (dMRI) study (Madsen et al. 2010). Inhibition capabilities are also known to be part of multiple complex cognitive construct such as impulsive behavior and attentional skills (Bari and Robbins 2013). Attention-deficit and impulsive behavior are major limitations in an individual's everyday life and activities, mostly in school-aged children. As an example, adults with attention-deficit–hyperactivity disorder (ADHD) are less likely to have graduated from college compared with controls, reflecting a major impact of these deficits on educational performance (Biederman et al. 2012). The impact of attentional deficits and impulsive behaviors on everyday activities are mostly evaluated using clinical diagnoses such as ADHD, borderline personality disorder and Tourette syndrome (Puiu et al. 2018). Recently, the National Institute of Mental Health urged researchers to evaluate cognitive functions outside of criteria-defined

Received: February 25, 2022. **Revised:** April 19, 2022. **Accepted:** April 20, 2022.

diagnostic syndromes as part of their Research Domain Criteria initiative. This article is a part of this new initiative as it aims to uncover and understand the structural neuroanatomy underlying attention deficit and impulsive behaviors in a general population of school-aged children while ignoring possible diagnosis.

Several previous studies in this field have evaluated the attentional and impulsive performance in ADHD patients, a very common disorder, affecting 3–8% of school-aged children and persisting into adulthood in 65% of cases (Rubia et al. 2014; Polanczyk et al. 2015). As with other psychiatric disorders, ADHD diagnosis is based solely on subjective evaluations from either parents, teachers, and/or clinicians as described in the DSM-5 manual, an approach that does not describe underlying neuroanatomical and physiological mechanisms that give rise to the cognitive and behavioral manifestations (Rubia et al. 2014; Posner et al. 2020). In response to the variability and heterogeneity of this "syndromic" approach, there is potential for neuroimaging techniques such as MRI to elucidate the functional and structural neuroanatomy behind ADHD (Rubia et al. 2014). Many studies have addressed the structural differences between ADHD patients and controls reporting a volumetric reduction in total brain volume and total gray matter (GM) volume including differences in the prefrontal, frontal, occipital, and parietal areas while divergent results have been reported concerning total white matter (WM) volume (Valera et al. 2007; Hutchinson et al. 2008; Narr et al. 2009; Nakao et al. 2011; Greven et al. 2015; Norman et al. 2016; Silk et al. 2016; Ambrosino et al. 2017; Hoogman et al. 2017). Volumetric reductions have also been reported in the basal ganglia region, mostly in the putamen, globus pallidum, and caudate nucleus (Valera et al. 2007; Ellison-Wright et al. 2008; Nakao et al. 2011; Frodl and Skokauskas 2012; Norman et al. 2016). Differences and delays in development of cortical thickness and surface area have been reported from structural studies, mostly in the prefrontal, frontal, parietal, temporal, and left occipital lobes (Shaw et al. 2007; Narr et al. 2009; Almeida et al. 2010; Shaw et al. 2012; Silk et al. 2016). Consistent with the findings from structural studies, researchers using task-based or resting state functional MRI have frequently reported the implication of the inferior frontal and superior frontal gyri, the supplementary motor area, and the basal ganglia in the neurophysiology of ADHD (Cortese et al. 2012; Hart et al. 2013; McCarthy et al. 2014; Lei et al. 2015). An increase in the activation of the default mode network has also been claimed in the neurophysiology of ADHD in various studies (Sonuga-Barke and Castellanos 2007; Cortese et al. 2012; Lei et al. 2015).

With the advent and refinement of dMRI in the last decades, researchers have turned their focus from the functional activity of GM to networks of WM fibers connecting these various regions implicated in the neurophysiology of ADHD. In a review oriented to clinicians, authors have listed many bundles thought to be implicated in the neurophysiology of ADHD. These bundles comprise the superior longitudinal fasciculus, corticospinal bundle, fornix, and bundles connecting the striatum, cerebellar, corpus callosum, corona radiata, internal capsule, occipital, and frontal lobe (Cortese et al. 2012). When evaluating the relationship between WM microstructure and attention and impulsivity/hyperactivity performance in children, researchers have identified bundles such as the thalamic radiation, corticospinal tracts, forceps minor, and bundles connecting regions of the parietal, occipital, orbitofrontal, and prefrontal lobe (Qiu et al. 2012; Cao et al. 2013; Hong et al. 2014; Y.-H. Wu et al. 2014b; Cha et al. 2015; Ameis et al. 2016; Zhan et al. 2017; Lin et al. 2020; Sudre et al. 2020). Although many bundles present strong associations, results are still heterogeneous and are highly dependent on the assessment method of attention and impulsivity in children. In addition, the use of diffusion tensor imaging (DTI)-derived measures in these studies does not allow for direct interpretation of the physiological context in the brain since they are not specific to any biological properties and are not robust to crossing populations that represents 90% of the brain's WM voxels (Jones 2010; Jeurissen et al. 2013; Jones et al. 2013). Better understanding of WM connectivity will provide information on the large-scale neuronal networks linking relevant regions of the cortex. In addition, extracting the local association fibers, which are underrepresented in dMRI studies due to extreme methodological challenge (Movahedian Attar et al. 2020) and evaluate how changes in this microstructure could underly attention and impulsive behavior in children.

This article goes beyond these limitations by (i) using validated psychometric tests to measure attention and impulsive behavior in a population-based cohort of school-aged children instead of a syndromic diagnostic approach and (ii) by using a state-of-the-art connectivity pipeline based on the Brainnetome atlas allowing the extraction of specific WM connections and (iii) by using dimensionality reduction techniques to obtain biologically interpretable WM measures. The Brainnetome parcellation is based on functionally driven criteria, allowing for better interpretation of the connection's function. The use of the whole-brain approach combined with the atlas allows for an inclusive approach rather than a limited predefined region of interest. We aim to elucidate, on a structural level, not only which connections are associated with attention and impulsive behavior but how alterations in the WM microstructure are related to these cognitive functions. In addition, we aim to uncover the localization of the WM alterations along each identified connection. We hypothesize that WM connections connecting the frontal lobe to the basal ganglia nuclei will be more represented considering the previous consistent association with response inhibition, a strong influencer of attention and impulsivity. In addition, we hypothesize that changes in microstructure

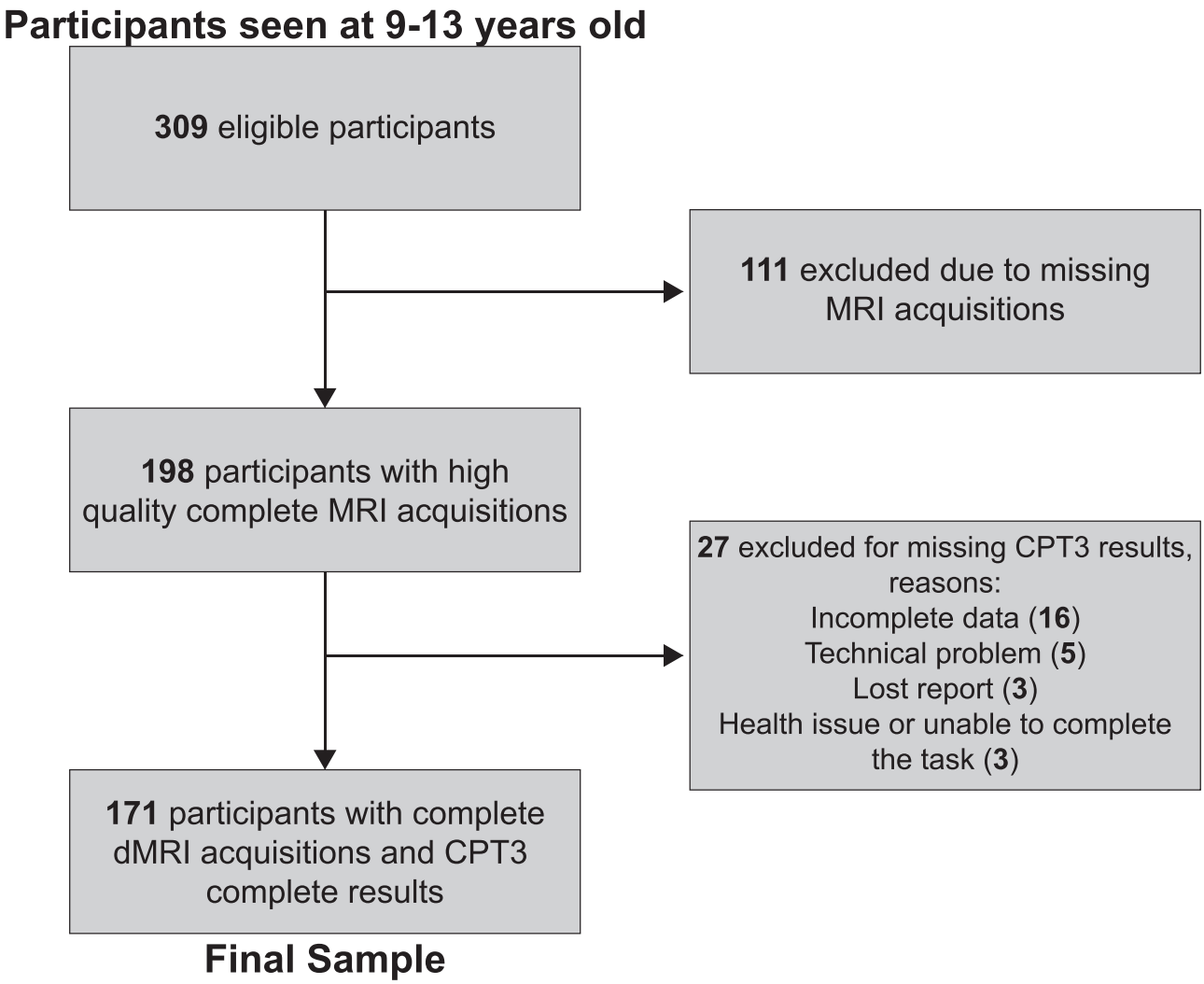

Fig. 1. Flowchart of total population with exclusion reasons.

reducing the capacity of information transmission in these WM fibers will be linked with a reduced attentional performance or control of impulsive behavior.

Methods

Study population

Participants are from the population-based cohort GESTation and Environment (GESTE) in Sherbrooke, Quebec, Canada. Recruitment was done between 2007 and 2009 and women during the first trimester of pregnancy or at delivery were enrolled ($n = 800$). Initial inclusion criteria were women aged ≥18 years, no known thyroid disease and no use of medication affecting thyroid hormone level. Data were collected over 4 waves, with the fourth currently in progress. In the fourth follow-up, children, aged 9–13 years old, are undergoing complete psychometric tests, including the Conners Continuous Performance test 3 (CPT3) to measure attention and impulsive behavior, and dMRI acquisition. Total sample size consisted of 309 children who participated in the fourth wave of the GESTE cohort. From these participants, 198 had high-quality dMRI acquisition and 171 had complete CPT3 results combined with high-quality dMRI (Fig. 1). Of these participants, 27 children had a clinical diagnosis of ADHD and 3 had a diagnosis of autism spectrum disorder (ASD). At the time of visit, 5 children were under ADHD medication and 23 children had taken ADHD or other psychotropic medications during the year prior to the visit. Study protocols were approved by both the Institutional Ethics Boards of the University of Sherbrooke and Columbia University.

Image acquisition

A 3-T whole-body scanner using a 32-channel head coil (Ingenia, Phillips Healthcare) was used to provide T1-weighted and single-shell high-angular resolution diffusion imaging (HARDI) acquisitions. Parameters for the T1-weighted structural acquisitions were: T1 3D TFE (Turbo Field Echo) pulse sequence, 8° flip angle, field of view (FOV) 240 mm, matrix size 240 × 240, slice thickness 1 mm. For the single-shell HARDI acquisition, the parameters were: $b = 1500$ mm/s^2, 68 volumes (64: $b = 1500$ mm/s^2, 4: $b = 0$ mm/s^2), FOV 230 mm, and voxel size of 1.8 mm isotropic.

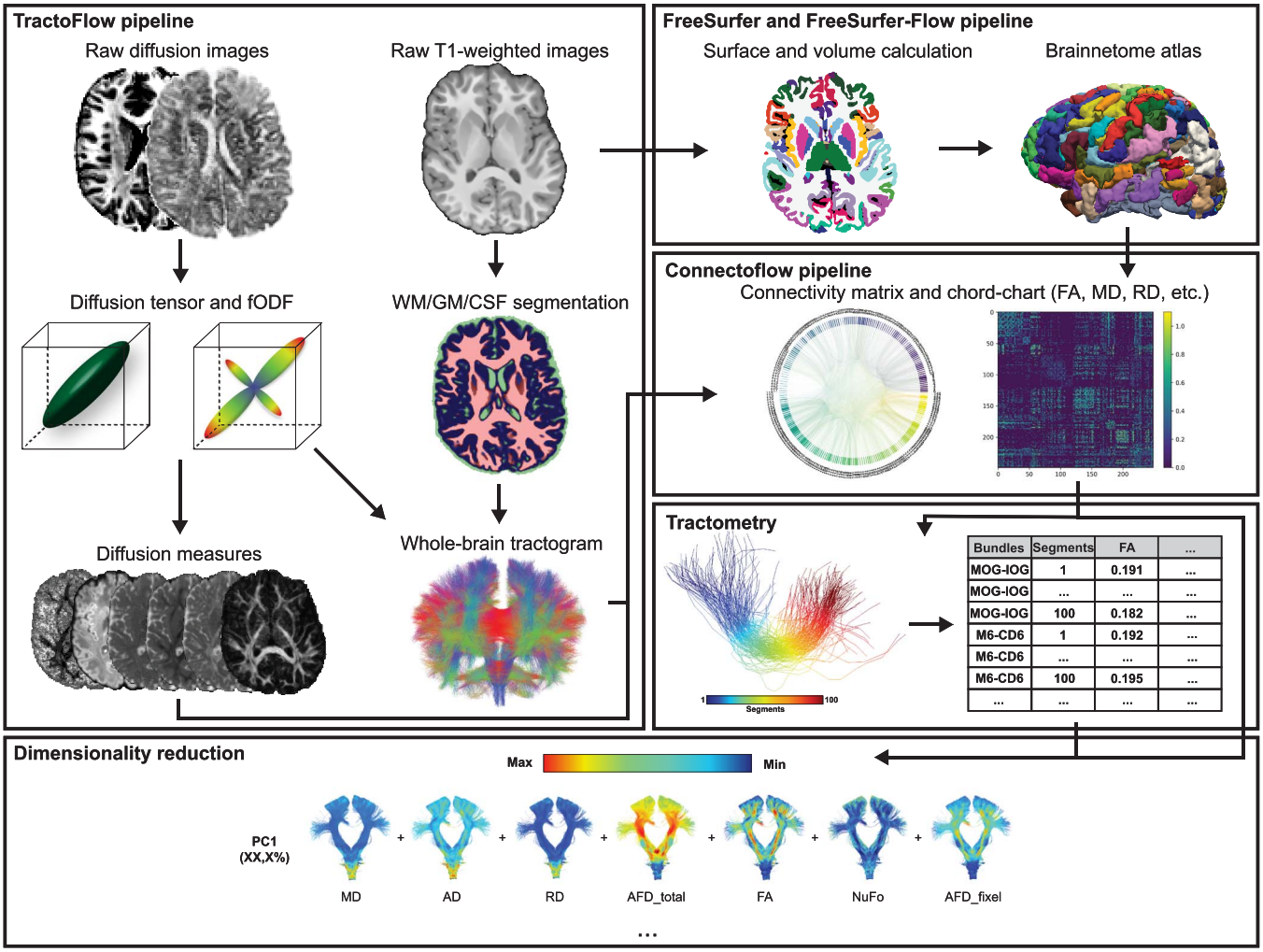

Fig. 2. Overview of the preprocessing and processing steps.

Diffusion-weighted image processing

Full processing steps can be seen in Fig. 2. To evaluate quality of acquisitions, visual quality control (QC) of raw images was performed on all participants, removing acquisitions with artifacts, slice dropping, or strong head motion. Diffusion-weighted images were processed using the Tractoflow pipeline (Jenkinson et al. 2012; Garyfallidis et al. 2014; Di Tommaso et al. 2017; Kurtzer et al. 2017; Tournier et al. 2019; Theaud et al. 2020; Avants et al. 2009) (https://github.com/scilus/tractoflow), an automated and reproducible pipeline allowing the computation of all the diffusion-related measures. Denoising, correction for eddy current and motion correction, correction for diffusion distortion, N4 correction, and intensity normalization were applied to raw images as part of this pipeline before computing the diffusion models. Measures such as fractional anisotropy (FA), mean diffusivity (MD), radial diffusivity (RD), and axial diffusivity (AD) were computed from the diffusion tensor model (Basser and Pierpaoli 1996). Measures such as the apparent fiber density (AFD_{tot}), number of fiber orientation (NuFO), and apparent fiber density specific to one population of fibers (AFD_{fixel}) were computed using the fiber-oriented distribution function (fODF), which were estimated from the constrained spherical deconvolution (Descoteaux et al. 2007; Tournier et al. 2007). Probabilistic tractography was then performed using 10 seeds per voxel to generate the full-brain tractogram based on the WM/GM maps (Descoteaux et al. 2009). Following the tractography, visual QC was performed on all subjects to ensure the quality of the resulting maps, metrics, and tractograms.

T1-weighted image processing

T1 images are visually examined to prevent acquisitions with artifacts or head motion before the beginning of the processing steps. To perform tractography, denoising, N4 correction, brain extraction, registration in diffusion space, and segmentation have been applied to raw images before computing the tracking maps as part of the TractoFlow pipeline.

To generate brain parcellations, the T1 volumes have been processed using the FreeSurfer pipeline (version 6.0, run with 3 T data option) on the CBRAIN web-based computing platform allowing segmentation of the cortical and subcortical areas, as well as volume and

surface statistics per parcellation (Fischl 2012; Sherif et al. 2014). Using a custom pipeline (https://github.com/scilus/freesurfer_flow), we further divided brain regions according to the Brainnetome atlas resulting in 249 brain parcellations (Fischl 2012; Fan et al. 2016; Di Tommaso et al. 2017; Kurtzer et al. 2017).

Segmentation of the tractogram

Combining the Brainnetome atlas with the full-brain tractogram, we performed WM connection extraction using the state-of-the-art Connectoflow pipeline (https://github.com/scilus/connectoflow) (Di Tommaso et al. 2017; Kurtzer et al. 2017). Connectoflow is a connectomic pipeline that automatically extracts streamline connecting 2 different parcels of interest (ROIs). This pipeline extracts connection-specific FA, MD, RD, AD, AFD_{tot}, NuFO, and AFD_{fixel} metrics from the whole-brain tractogram based on the atlas' parcels. Resulting connections are filtered for outliers, length, and looping angles in the same manner that classical bundles are filtered after their extraction and are registered in MNI space to compute a similarity metric for each connection across all subjects. Using this whole-connectome approach allows us to identify connections that rely on functionally driven sub-cortical and cortical parcels rather than known well-defined classical WM bundles.

Tractometry

To perform connection-profiling, we used the Tractometry-flow pipeline (https://github.com/scilus/tractometry_flow) to further divide significant connections into 100 sub-sections (Yeatman et al. 2012; Cousineau et al. 2017; Di Tommaso et al. 2017; Kurtzer et al. 2017). Diffusion measures such as AD, MD, FA, RD, AFD_{tot}, NUFO, and AFD_{fixel} were computed individually for each subsection further concatenated in a single dataset to apply dimensionality reduction. Graphical representation of each component presents the evolution the WM microstructure along the connection allowing the localization of the main difference between 2 conditions. One cluster of connection's subsections were considered as significantly different if 5 or more closely localized subsections presented P-value < 0.05. Using this number as a threshold allows us to reduce the false positive bias as 5 sub-sections represent 5% of the connection sub-sections. This ensures robustness of our findings without using too conservative multiple comparisons methods.

Dimensionality reduction

Classic diffusion measures such as DTI metrics are common in the literature but are highly correlated with one another and difficult to interpret in relation to the true biological situation. To overcome this limitation, it has been proposed by Chamberland *et al.* to reduce dimension of diffusion measures to improve tractometry of the WM connections (Chamberland et al. 2019). We performed standardization of all diffusion measures to a common scale and validation of suitability of our sample (Kaiser–Meyer–Olkin, KMO > 0.6 and sphericity $P < 0.05$). We performed principal component analysis (PCA), using scikit-learn python library (Pedregosa et al. 2011), on all complete connection diffusion measures (FA, RD, MD, AD, AFD_{tot}, NuFO, and AFD_{fixel}) for all connections detected in every subjects to extract significant components. Only components with eigenvalues superior to 1 were conserved as true component for multivariate regression analysis. In addition to this first PCA analysis, we performed a second dimensionality reduction approach using the same steps and criteria on only the sections-specific metrics resulting from the tractometry processing steps. Connections incorporated in this analysis were the connections-of-interest resulting from the group comparison analysis.

Statistical analysis

All statistical analysis has been performed in Python. We performed factorial analysis with oblimin rotation and minimal residual method using the Factor_analyzer python library (https://github.com/EducationalTestingService/factor_analyzer) on raw CPT3 variables to extract factors corresponding to attention and impulsivity. We validated the suitability of our sample by performing the KMO test and the Bartlett's test by using threshold values of >0.60 for the KMO test and a P-value < 0.05 for the Bartlett's test. Factors yielding eigenvalues superior to 1 were identified as true factors. Transforming data according to the factors, we extracted 2 groups per factor corresponding to poor performer (20% lower attention/impulsivity) and good performer (20% high attention/impulsivity). We then compared each diffusion measures between the 2 groups of subjects at each end of the spectrum for both impulsivity and attention using a 2-tailed unpaired t-test. Connections were first identified as significant if P-value < 0.05. To replace the use of too conservative multiple comparison corrections, we then filtered significant connections by conserving only the ones that were significant across 1 or more DTI measures (FA, MD, RD, and AD) and that were significant for the NuFO, AFD_{tot}, and AFD_{fixel} while being present in every subject from our population. These filtering criteria ensure the robustness of the identified connections by considerably reducing their numbers ($\sim$2000 to 10 connections). Following the tractometry processing, using the same groups, connection profiling was performed by computing the mean and standard deviation (SD) of each subsection from both groups. In order to evaluate significant difference, we performed a 2-tailed t-test between the mean of both groups on each subsection. Subsections were considered significantly different if P-value < 0.05.

Following the connectome-wide and connection profiling analysis, for each connections meeting the previous conditions, we performed multiple linear regression (MLR) analysis between the extracted principal components (PCs) from dimensionality reduction and attention/impulsivity score using the Statsmodels python library (Seabold and Perktold 2010). Two separate MLR

Table 1. Study population characteristics.

	N (%)	SD		Age range (years)					
Sex									
Male	104 (60.8)			(9.12–13.27)					
Female	67 (39.2)			(9.45–13.33)					
Total	171								
Age	11.33	±	1.31	(9.12–13.33)					
IQ	103.25	±	11.12						
Handedness									
Right	152 (88.9)			(9.30–13.33)					
Left	19 (11.1)			(9.12–13.00)					
Diagnosis									
ADHD	27 (15.8)			(9.47–12.61)					
Male	18 (66.7)			(9.47–12.61)					
Female	9 (33.3)			(10.58–12.36)					
ASD	3 (1.8)			(10.76–12.21)					
Gestational age (weeks)	39.02	±	1.52						
Birth weight (g)	3362.37	±	506.51						
Moderate to late preterm (32–37 weeks)	6 (3.51)								
Maternal alcohol in pregnancy [a]	44 (25.7)								
Smoking in pregnancy	12 (7.0)								
Family income (CAD$)	110,399	±	70,926						
Parental ADHD	34 (19.9)								
	No diagnosis (144)			**ADHD (27)**			**ASD (3)**		
CPT3 scores (±SD)									
Detectability	57.61	±	7.29	58.44	±	7.81	58	±	6.08
Omission	63.15	±	13.65	64.85	±	14.38	62.33	±	15.04
Commission	52.42	±	7.43	52.67	±	6.72	53.67	±	7.51
Perseverations	56.47	±	12.91	60.3	±	14.35	56.67	±	9.61
HRT	50.75	±	8.35	52.56	±	10.15	50.67	±	3.06
HRT SD	58.54	±	12.28	62.44	±	11.93	58.67	±	3.06
Variability	56.28	±	13.59	58.33	±	11.95	51.33	±	5.13
HRT block change	52.05	±	10.65	51.19	±	10.96	62	±	23.07
HRT inter-stimulus interval (ISI) change	55.28	±	10.35	57.85	±	12.87	57.33	±	11.59

[a]No heavy consumers.

analyses were conducted, the first time with and second time without children presenting a diagnosis to validate if the variability in cognition was explained solely by the presence of diagnose children. The covariates used in the MLR analysis were subject's age, biological gender, IQ (obtained from the WISC-IV global component), and handedness (define as self-reported dominant hand). Associations were significant if P-value was <0.05.

Results

Study population

From the initial 309 eligible participants, 171 participants have been included in this analysis (Fig. 1).

Summary table of the population characteristics can be seen in Table 1. Average age is 11.34 (±1.50) years old for the male participants and 11.31 (±0.95) years old for the female participants. Mean IQ of the study population is 103.25 (±11.12) and 88.9% of the participants are right-handed. Of the 27 participants diagnosed with ADHD, 18 are male and 9 are female. As shown in Table 1, no significant differences between the raw CPT-3 scores of each group have been observed in our population. This suggests that children with a diagnosis can present the same performance score as neurotypical children.

CPT3 factorial analysis

First and second factor yielded eigenvalues of 4.23 and 1.92, respectively. Hit reaction time (HRT) SD, variability, omission, and HRT interstimulus interval change were the variables with the highest loadings for the first factor (0.99, 0.84, 0.71, and 0.58, respectively). Commission, HRT, detectability, and perseverations were the variables with the highest loadings for the second factor (0.76, −0.69, 0.67, and 0.41, respectively). Detailed loadings and eigenvalues can be seen in Table 2. Observing the contributions of each score to the factors, we identified the first factor as the attentional skills score and the second factor as the impulsive behavior score.

Connection identification

The initial group comparison analysis yielded nearly 2000 significant connections between groups with higher

Table 2. Eigenvalues and loadings for the 2 factors resulting from the factorial analysis of the CPT3.

	Factor 1	Factor 2
Eigenvalues	4.23	1.92
Loadings		
Detectability	0.551	0.671
Omission	0.712	0.068
Commission	0.165	0.757
Perseverations	0.514	0.410
HRT	0.570	-0.691
HRT SD	0.998	0.003
Variability	0.841	0.084
HRT block change	0.397	-0.269
HRT ISI change	0.576	-0.139

and lower performance score. Following filtering steps, the analysis yielded 2 significant connections for the attentional score and 8 significant connections for the impulsivity score. Connections between the right area 41/42 and right rostroventral area 40 (A41/42–RA40) and right middle occipital gyrus and right inferior occipital gyrus (MOG–IOG) were associated with attention score (Fig. 3). Connections between the right medial area 6 and right caudal dorsolateral area 6 (M6–CD6), right medial area 6 and right posterior parietal thalamus (M6–PPT), right area 46 and right lateral area 10(A46–LA10), left fusiform gyrus medioventral area 37 and left inferior occipital gyrus (FG37–IOG), left caudal lingual gyrus and left occipital polar cortex (CLG–OPC), left caudal cuneus gyrus to left medial superior occipital gyrus (CCG–MSOG), right nucleus accumbens and right occipital thalamus (NA–OT), and right dorsal caudate and right lateral pre-frontal thalamus (DC–PFT) were associated with impulsivity score (Fig. 3). Each connection was very closely spatially located in-between each subject when registered in a common space reducing the risk for false positive connection extraction (Table 3).

Dimensionality reduction

Dimensionality reduction of connection metrics yielded 2 PCs with eigenvalues superior to 1. The first PC explained 77.7% (eigenvalue = 5.44) of the variance contained in all diffusion metrics and the second component explained 18.6% (eigenvalue = 1.30) of total variance (Fig. 4A). MD, AD, and RD had the 3 highest loadings for the first PC (0.425, 0.422, and 0.416, respectively) and AFD_{fixel}, FA, and NuFo had the 3 highest loadings for the second PC (0.866, 0.334, and −0.276, respectively) (Fig. 4A). Based on metrics contribution, we interpreted the first PC as a metric of microstructural complexity and the second PC as a metric for axonal density. Dimensionality reduction of sub-sections metrics yielded similar PCs in the reverse order such as PC1 showed a high contribution of FA, AFD_{fixel}, and RD metrics (−0.496, −0.442, and 0.442, respectively) as opposed to PC2 with contribution of mostly MD, AD, and AFD_{total} metrics (0.645, 0.521, and −0.431, respectively) (Fig. 4B). PC1 was interpreted as axonal density and PC2 as microstructural complexity.

Relationship between WM microstructure and cognitive functions

When keeping children with diagnosis, multivariate regression analysis, using the complete connection PCs, showed that increased microstructural complexity was associated with a less impulsive behavior during the CPT3 on connections connecting the left area 46 and left lateral area 10 (A46–LA10), left fusiform gyrus medioventral area 37 and left inferior occipital gyrus (FG37–IOG), left caudal cuneus gyrus and left medial superior occipital gyrus (CCG–MSOG), and right dorsal caudate nucleus and right lateral pre-frontal thalamus (DC–PFT) while controlling for age, sex, handedness, and IQ ($\beta = -0.339$, $P = 0.0004$, $R^2 = 0.09$; $\beta = -0.230$, $P = 0.003$, $R^2 = 0.07$; $\beta = -0.166$, $P = 0.011$, $R^2 = 0.06$; $\beta = -0.182$, $P = 0.041$, $R^2 = 0.05$; respectively) (Table 3). In addition, increased axonal density was associated with a less impulsive behavior on connections between the right medial area 6 and right posterior parietal thalamus (M6–PPT), and right dorsal caudate nucleus and right lateral pre-frontal thalamus (DC–PFT) ($\beta = -0.392$, $P = 0.027$, $R^2 = 0.05$; $\beta = -0.359$, $P = 0.028$, $R^2 = 0.05$; respectively) (Table 3). No associations were found to be significant with attentional skills. The addition of an interaction between sex and WM microstructure was not significant and, therefore, not kept in the model.

When removing children with a diagnosis (ADHD or ASD), A46–LA10, FG37–IOG, and CCG–MSOG remained significant regarding the association between microstructural complexity and impulsive behaviors ($\beta = -0.287$, $P = 0.007$, $R^2 = 0.05$; $\beta = -0.178$, $P = 0.039$, $R^2 = 0.03$; $\beta = -0.241$, $P = 0.0006$, $R^2 = 0.09$, respectively) (Table 3). On the other hand, the association between microstructural complexity and impulsive behaviors did not remain significant on connection DC–PFT ($\beta = -0.095$, $P = 0.328$, $R^2 = 0.01$) (Table 3). Connection M6–PPT remained significant and connection M6–CD6 showed an association between higher axonal density et less impulsive behavior during the CPT3 ($\beta = -0.576$, $P = 0.004$, $R^2 = 0.06$; $\beta = -0.345$, $P = 0.018$, $R^2 = 0.04$, respectively) (Table 3). DC–PFT did not remain significant when removing children with diagnosis while examining the axonal density and impulsive behaviors ($\beta = -0.328$, $P = 0.055$, $R^2 = 0.03$, respectively) (Table 3). As for the attentional skills, no connections were found to be significant when removing children with a diagnosis.

Connection profiling

When evaluating only the endpoints of each connection, the group showing a more impulsive behavior during CTP3 had a significantly higher microstructural complexity in the endpoint of connection M6–CD6 (6 subsections, located between segment 1 and 11), whereas the group showing a less impulsive behavior had a significantly higher axonal density in the endpoint of

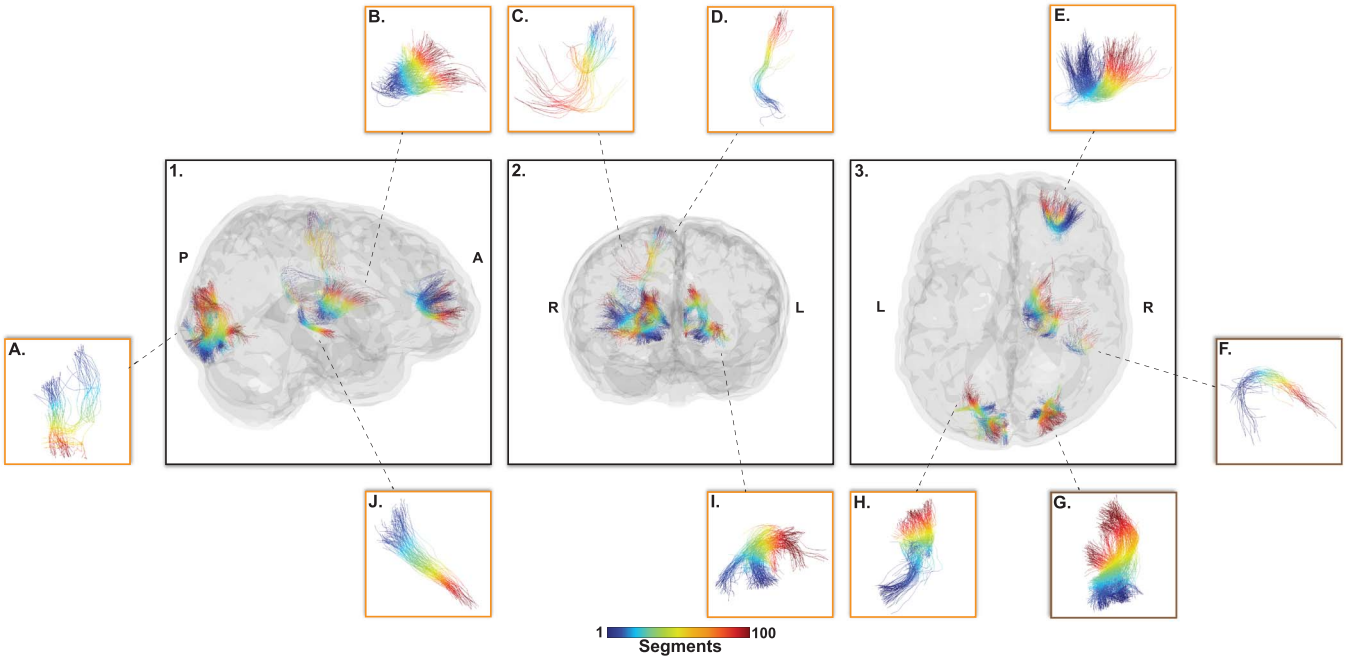

Fig. 3. Top-10 connections-of-interest that survived the filtering steps from the group comparison analysis (20% higher score vs 20% lower scores). These connections present significant difference on at least 1 DTI metrics (FA, MD, RD, AD) and AFD_{fixel}, AFD_{total}, and NuFo as well as being present in every subject from our population. Orange box identifies connections significant for impulsivity and brown box for attention. A) CLG–OPC, B) DC–PFT, C) M6–CD6, D) M6–PPT, E) A46–LA10, F) A41/42–RA40, G) MOG–IOG, H) CCG–MSOG, I) FG37–IOG, J) NA–OT. Color represents connections' sub-sections.

Table 3. Results controlled for age, sex, handedness, and IQ from the multivariate regression analysis across all subjects ($n = 171$).

Connections	Microstructural complexity				Axonal density				Similarity$^{\omega}$ (mm)
	N	β (95% CI)	P	R^2	N	β (95% CI)	P	R^2	
With diagnosis									
Attention									
A41/42–RA40	171	−0.08 (−0.19 to 0.04)	0.215	0.03	171	0.29 (−0.01 to 0.58)	0.056	0.04	1.99
MOG–IOG	171	−0.14 (−0.28 to 0.001)	0.051	0.04	171	0.23 (−0.12 to 0.58)	0.200	0.03	3.00
Impulsivity									
M6–CD6	171	0.03 (−0.02 to 0.07)	0.261	0.03	171	−0.25 (−0.52 to 0.02)	0.070	0.04	3.03
M6–PPT	171	−0.08 (−0.17–0.02)	0.111	0.04	**171**	**−0.39 (−0.74** to **−0.04)**	**0.027**	**0.05**	1.99
A46–LA10	**171**	**−0.34 (−0.52 to −0.15)**	**0.0004**	**0.09**	171	−0.15 (−0.56 to 0.26)	0.463	0.03	1.59
FG37–IOG	**171**	**−0.23 (−0.38 to −0.08)**	**0.003**	**0.07**	171	−0.37 (−0.74 to 0.001)	0.051	0.05	2.32
CLG–OPC	171	−0.06 (−0.12 to 0.01)	0.099	0.04	171	−0.15 (−0.42 to 0.12)	0.263	0.03	2.41
CCG–MSOG	**171**	**−0.17 (−0.29 to −0.04)**	**0.011**	**0.06**	171	−0.20 (−0.55–0.15)	0.266	0.03	2.01
NA–OT	171	−0.12 (−0.27 to 0.03)	0.114	0.04	171	−0.16 (−0.43 to 0.10)	0.227	0.03	2.87
DC–PFT	**171**	**−0.18 (−0.36 to −0.01)**	**0.041**	**0.05**	**171**	**−0.36 (−0.68 to −0.04)**	**0.028**	**0.05**	1.07
Without diagnosis									
Attention									
A41/42–RA40	142	−0.05 (−0.18 to 0.08)	0.427	0.03	142	0.29 (−0.04to 0.62)	0.082	0.04	1.99
MOG–IOG	142	−0.11 (−0.25 to 0.04)	0.151	0.04	142	0.17 (−0.27to 0.60)	0.449	0.03	3.00
Impulsivity									
M6–CD6	142	0.02 (−0.03 to 0.07)	0.410	0.01	**142**	**−0.35 (−0.63 to −0.06)**	**0.018**	**0.04**	3.03
M6–PPT	142	−0.08 (−0.18 to 0.01)	0.092	0.02	**142**	**−0.58 (−0.96 to −0.19)**	**0.004**	**0.06**	1.99
A46–LA10	**142**	**−0.29 (−0.49 to −0.08)**	**0.008**	**0.05**	142	−0.26 (−0.70 to 0.18)	0.248	0.01	1.59
FG37–IOG	**142**	**−0.17 (−0.34 to −0.004)**	**0.044**	**0.03**	142	−0.28 (−0.69 to 0.12)	0.171	0.02	2.32
CLG–OPC	142	−0.07 (−0.14 to −0.001)	0.047	0.03	142	−0.09 (−0.38 to 0.19)	0.525	0.006	2.41
CCG–MSOG	**142**	**−0.24 (−0.38 to −0.11)**	**0.0006**	**0.09**	142	−0.33 (−0.73 to 0.08)	0.110	0.02	2.01
NA–OT	142	−0.12 (−0.28 to 0.04)	0.151	0.02	142	−0.16 (−0.44 to 0.12)	0.268	0.01	2.87
DC–PFT	142	−0.09 (−0.28 to 0.10)	0.328	0.01	142	−0.33 (−0.66 to 0.007)	0.055	0.03	1.07

ω: Mean space localization across subjects (mm), 0–4 mm: very close, 4–8 mm: similar, 8–12 mm: very different. Bold: Significant association

connection A46–LA10, FG37–IOG, and DC–PFT (6 subsections (1–8), 10 subsections (1–15), and 7 subsections (94–100), respectively) (Fig. 5). When focusing on clusters located in the connection core, children showing a more impulsive behavior had significantly higher microstructural complexity on connection FG37–IOG, CCG–MSOG, NA–OT, and DC–PFT (11 subsections (30–43), 24 subsections (46–75), 15 subsections (71–86), and 9 subsections

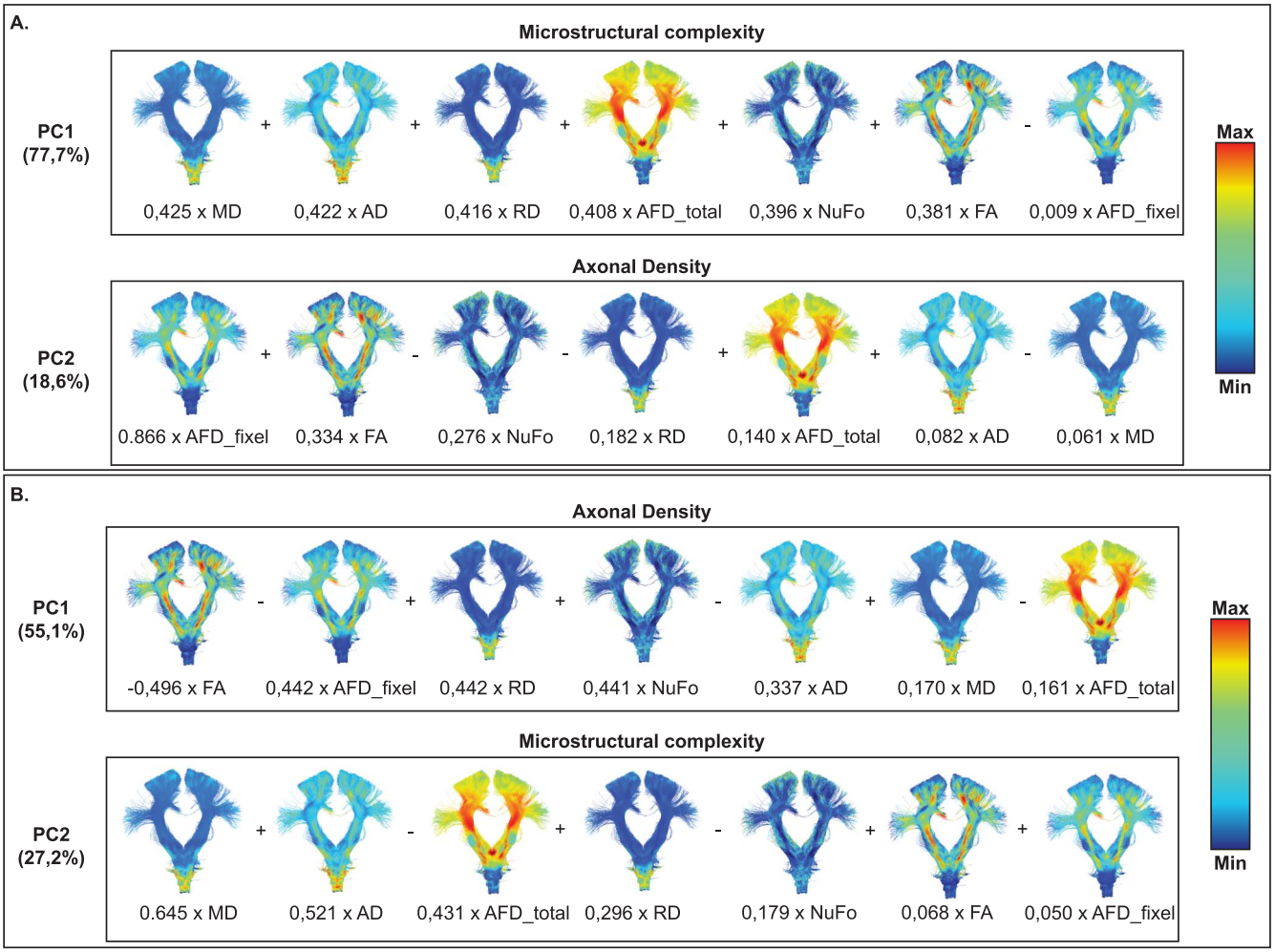

Fig. 4. Results from dimensionality reduction analysis using in A) complete connection PCs (whole connection metrics) and B) sub-section PCs (based on the sub-sections specific metrics). Connections are colored from anatomy-based metric.

(59–72), respectively). Children with a less impulsive behavior had a significantly higher axonal density on cluster located in the core of connection CLG–OPC and DC–PFT (7 subsections (15–27) and 7 subsections (42–52), respectively). No statistically significant differences were found between groups showing good or poor attentional skills for axonal density or microstructural complexity.

Discussion

Localization of reported connections

This study identified multiple WM connections associated with attentional skills and impulsive behaviors as well as the impact of the WM microstructure on these cognitive functions in a population of school-aged children. We previously hypothesized that most identified connections would be between the frontal lobe and basal ganglia. The use of a connectome-wide approach allowed us to consider the entirety of the WM tracts connecting all cortical and subcortical parcellations of the Brainnetome atlas. This approach allows the evaluation of WM connections that are not often seen in dMRI studies, since they are not comprise within main WM bundles. For impulsive behaviors, our analysis identified 8 connections located in the prefrontal, parietal, occipital, temporal lobes, and basal ganglia. For attentional skills, we identified 2 connections between the MOG–IOG and the right area 41/42 and right rostroventral area 40. Connections in the occipital, temporal, and parietal lobe did not fully converge with our initial hypothesis, which could be explained by various factors: (i) attentional skills and impulsive behaviors are measured via visual response to a stimulus as part of the CPT3, which could explain why our analysis yielded connections implicated in the visual processing of the brain, mostly in the occipital lobe but also located in the temporal lobe (Goodale and Milner 1992); (ii) similar to the previous point, connections located in the parietal lobe are part of the somatosensory network that is essential when performing a response to a stimulus during the CPT3 (Smith 2021). As attentional skills and impulsive behavior are complex cognitive functions requiring pathways such as the visual and the somatosensory network, it is possible that both attention and impulsivity can be affected by the visual or somatosensitive processing. Although the connections in parietal, occipital, and

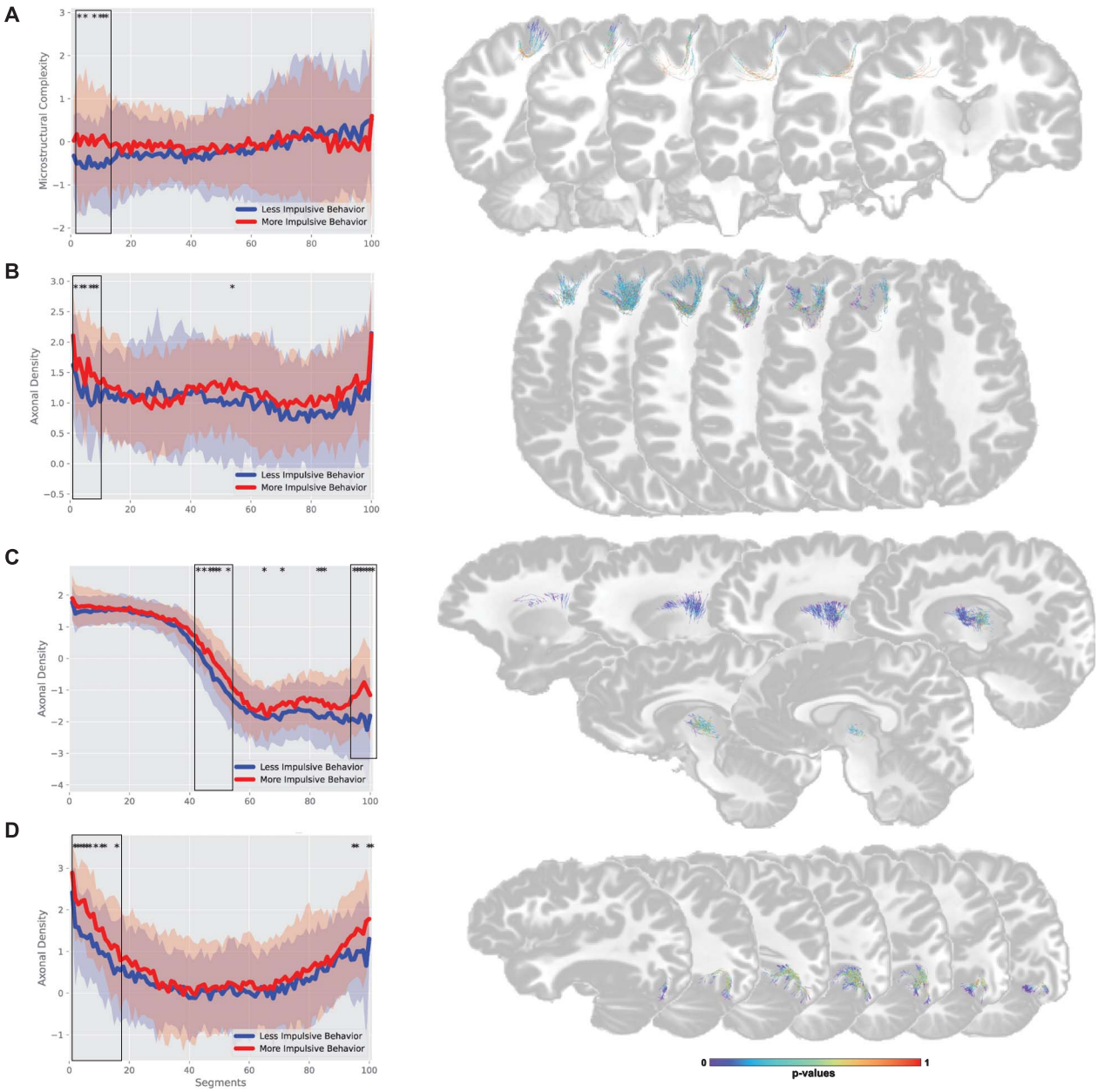

Fig. 5. Connection profiles comparison between the 20% higher performance and 20% lowest performance group. ∗: represent sub-sections were both groups are significantly different. Black rectangles represent clusters of significantly different sub-sections (defined as 5 or more closely localize significantly different sub-sections). Analysis was performed using the component extracted from the sub-sections specific metrics (results from tractometry). Axonal density is inverse scored, lower values = higher axonal density while higher values = lower axonal density. A) M6–CD6, B) A46–LA10, C) DC–PFT, D) FG37–IOG. Connection are colored based on *P*-values for each sub-sections.

temporal lobe have already been associated with various cognitive functions deficits, impulsivity is a complex cognitive construct that encompass many sub-dimensions. Having one connection associated with a unique cognitive function is highly unlikely when considering the complex interactions between the neuroanatomy and the cognitive functions. Therefore, a single WM fiber can be found implicated in various deficits due to the complex construct that impulsivity represents. As for the remaining connections, mostly located in the prefrontal, nucleus accumbens, dorsal caudate, and thalamus did converge with our initial hypothesis, reinforcing previously reported findings in the literature (Qiu et al. 2012; Cao et al. 2013; Hong et al. 2014; Y.-H. Wu et al. 2014b; Cha et al. 2015).

Strength and limitations

This study evaluates the WM microstructure distribution within a socially advantaged population of children from virtually healthy pregnancies with no or few risk factor for neurodevelopmental disorder allowing for extrapolation to general population. This is one of the major aspects that distinguish this approach compared

to a classical case–control approach. Due to the small number of studies assessing the validity of extracted "virtual" connections versus biological "post-mortem" tracts, it is difficult to validate the true existence of our computed connections in post-mortem studies. In an effort to assess the anatomical validity of our connections-of-interest and to add strength to our results, we (i) kept only connections present in 100% of our subjects and (ii) registered each connection in a common MNI space, allowing the measurement of the spatial localization of each connection in-between subjects symbolized as the similarity metric (Table 3). Every extracted connection yielded a similarity distance ranging from 0 to 4 mm. Thus, each extracted connections are anatomically valid WM tracts. On the other end, the scale from which we are measuring WM microstructure (imaging voxel is 1.8 mm^2 isotropic) does not allow for precise examination of more specific regions within the WM itself and therefore represent an important limitation to consider. Other strengths of this study include the use of dimensionality reduction technique allowing the extraction of more biologically interpretable components. In addition, the use of validated psychometric test combined with factorial analysis allowed us to better take into consideration the cognitive variability and create a more representative model of attention and impulsivity in our population-based children population. Although we accounted for major limitations, microstructural complexity and axonal density as components haven't been validated in carefully dissected WM tracts. In addition, the unavailability of previous follow-up MRI data removed the ability to evaluate WM developmental trajectories in our population.

Overlapping with "classical" WM bundles

When evaluating the location of our connections and due to their small size, it is interesting to evaluate if these connections can be comprised within "classical" WM bundles. The connection M6–CD6 overlapped with the right pyramidal bundle (PYT_R), the right fronto-pontine bundle (FPT_R), the right frontal aslant bundle (FAT_R), and the corpus callosum (pre/post central gyri (CC_Pr_Po) and posterior part of the frontal lobe (CC_Fr_2)) (Fig. 6A). The connection M6–PPT presented overlap with the PYT_R, FPT_R, and the right parieto-occipital pontine bundle (POPT_R) (Fig. 6B). The connection A46–LA10 showed overlap with the right uncinate fasciculus (UF_R), the right superior longitudinal fasciculus (SLF_R), the right inferior fronto-occipital fasciculus (IFOF_R), FPT_R, the right cingulum (CG_R), the corpus callosum (anterior part of the frontal lobe (CC_Fr_1)), and the right arcuate fasciculus (AF_R) (Fig. 6C). The connection A41/42–RA40 was overlap by only the AF_R (Fig. 6D). All connections located in the occipital lobe (FG37–IOG, CLG–OPC, CCG–MSOG, and MOG–IOG) were overlap by the optic radiation and Meyer's loop (OR_ML), the inferior longitudinal fasciculus, the IFOF and the corpus callosum (occipital lobe (CC_Oc)) (Fig. 6E–H). The connection NA–OT was overlap by the optic radiation and Meyer's loop (OR_ML), whereas the connection DC–PFT was overlap by the right superior cerebellar peduncle (SCP_R), the PYT_R, and the FPT_R (Fig. 6I–J). Considering the variety of overlap with "classical" WM bundles, it is possible that they are normally extracted as part of these bundles and therefore hidden within these main WM pathways.

Psychometric assessment

One strength of this study is the assessment method of attentional skills and impulsive behavior. When looking at the raw score in the CPT3, we can observe that there are no significant differences between each group (e.g. ADHD, ASD, no diagnosis) reinforcing the need of evaluating cognitive function outside the diagnosis criteria. This observation also brings confidence to our previous reported connections, as one could argue that the difference between the 2 groups is generated by the children with a diagnosis. As stated in the literature, most studies use exclusively questionnaires administered to the parents, teacher, or clinicians, perpetuating the clinical heterogeneity of this syndromic approach of the current ADHD diagnosis method (Rubia et al. 2014; Posner et al. 2020). While some studies use psychometric test such as the CPT3, they often use only one test metric as the attention score or the impulsivity score, which also introduces a bias since attentional deficit and impulsive behavior can be expressed in multiple different ways. It has been suggested by some research group that combining CPT3 scores would significantly improve classification accuracy (Ord et al. 2021); meanwhile others have claimed that composite scores did not improve the classification accuracy when comparing to individual measure (Scimeca et al. 2021). Even though there is no clear answer currently, factorial analysis, when interpreted with caution, can allow us to better evaluate attention and impulsivity deficits by considering every score obtained from the CPT3 according to their respective weight. The first factor was identified as the attentional skills based on the high contribution of the omission and HRT SD score, whereas the second factor was identified as the impulsive behaviors based on the high contribution of the commission score, which are often use individually as attention or impulsivity metric in various studies, thus adding an objective performance analysis for these cognitive functions in our study (Epstein et al. 2003; Hong et al. 2014).

Beyond DTI metrics and PCA

As mentioned above, the use of DTI metrics to assess WM integrity introduces an important limitation as it cannot discriminate voxel containing crossing, merging, or kissing fibers (Jones 2010; Jeurissen et al. 2013; Jones et al. 2013). To overcome this limitation, the use of a novel metric, AFD_{fixel}, was used in order to provide information specific to only one fiber population (Raffelt et al. 2017).

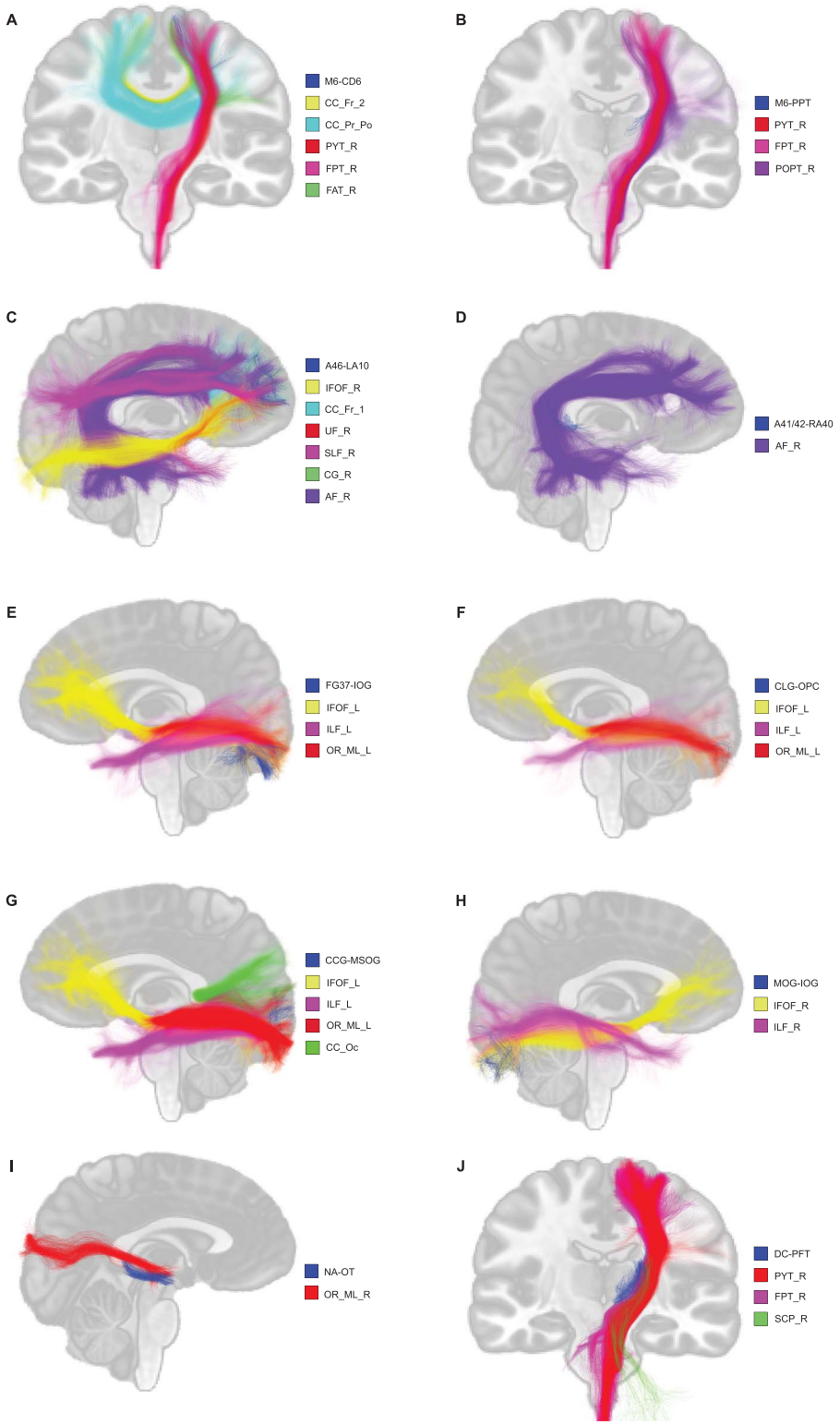

Fig. 6. Visual representation of connections overlapping with "classical" WM bundles. A) M6–CD6, B) M6–PPT, C) A46–LA10, D) A41/42–RA40, E) FG37–IOG, F) CLG-OPC, G) CCG–MSOG, H) MOG–IOG, I) NA–OT, J) DC–PFT.

In addition, a novel approach of dimensionality reduction of diffusion data was applied, allowing the extraction of more biologically relevant and interpretable measures (Chamberland et al. 2019). As a result, the first PC from the connection PCA analysis explained 77.7% of the total variance and was identified as representing the microstructural complexity since mostly non-fiber-specific metrics, such as DTI metrics, were equally contributing to this component while AFD_{fixel} did not (Fig. 4A). On the other hand, the second PC, explaining 18.6% of the total variance, showed contribution of mostly exclusively the AFD_{fixel} metric, therefore

identified as axonal density (Fig. 4A). Both PCs converge with previously reported results from a pediatric population using the same diffusion metrics but diverge from results reported in 2 other studies using a more extended panel of diffusion measures in a typically developing pediatric population (Chamberland et al. 2019; Geeraert et al. 2020; Guberman et al. 2021). Interestingly, connection sub-sections dimensionality reduction extracted similar PCs, but in a reverse order (Fig. 4B). Although counter-intuitive, creating a connection profile based on a high number of sub-sections (100 sub-sections per connection here), as opposed to a measure reflecting the mean of an entire connection, should reflect measure influenced more by the connection itself. When segmenting a connection, the probability of obtaining a segment encompassing only the connection fibers and not crossing fibers is higher than on a whole connection level. Therefore, more sub-sections reflect measures specific to the connection than sub-sections reflecting an intersection of crossing fibers influencing the results from the PCA analysis. Therefore, it is not surprising that the microstructural complexity was extracted as the second PC explaining 27.2% of the total variance compared with 55.1% for the axonal density as a larger proportion of the evaluated sub-sections represents connection-specific metrics (Fig. 4B).

Microstructural complexity implication in impulsive behavior

Due to the various contributions of diffusion measures in each PCs, interpretation of the multivariate linear regression analysis is not easily comparable with other studies as this is, to our knowledge, the first time this technical approach has been used in a pediatric population to understand the relationship between WM and attention/impulsivity. However, our results show consistent associations between higher microstructural complexity and less impulsive behavior, which could be seen as an increase in the presence of glial cells, myelin, and crossing fibers. Glial cells being implicated in multiple functions such as myelin production, neurotransmitters recycling, neuronal repair, and nutrients sourcing and storage (Mayorga-Weber et al. 2022), it is likely that a well-supported connection of axons present a higher capacity of transmitting information between regions of the cortex. Therefore, efficient connections can translate to better inhibitory capabilities thus reducing the impulsive behaviors that can be seen in children presenting lower microstructural complexity. However, microstructural complexity, as a component, is still for the most part a model representation based on classical diffusion metrics and has not yet been validated in careful WM dissection post-mortem studies. To add support to this hypothesis, studies reported negative associations between RD or/and AD metrics, which are contributing greatly to the microstructural complexity component, and hyperactivity/impulsivity symptoms severity in ADHD children (Sudre et al. 2020). Previous study showed associations often between symptom severity and FA values, which is thought to reflect mostly a high myelin density and a tight orientation profile of WM fibers but with the caveat, as previously stated, of limited capacity for discerning crossing, kissing, or merging fibers (Jeurissen et al. 2013; Seehaus et al. 2015).

Our results converge with the previously reported decrease in FA values on the callosal tracts in ADHD girls compared with controls (Lin et al. 2020) and the connection connecting the left superior occipital gyrus and the left precuneus in ADHD children when evaluating the association with the CPT3 commission score, probably reflecting the visual components of this test (Hong et al. 2014). In a voxel-based study, FA reduction in the sagittal striatum, posterior thalamic radiation, and body and splenium of the corpus callosum was associated with a higher hyperactive/impulsive rating, which converges with our present results (Qiu et al. 2012). Even though these studies have differences in term of symptom assessment, ROIs, and processing techniques, they provide confidence in our result by reporting the same directionality in their association between impulsive behavior and diffusion metrics.

Axonal density implication in impulsive behavior

The interpretation of the second PC, axonal density, is easier than the microstructural complexity, as it reflects mostly the AFD_{fixel}, an indicator of axon density specific to 1 fiber population (Raffelt et al. 2017). Our results still show consistent association between higher axonal density and less impulsive behavior as it can be simply interpreted as a higher axonal density translate to better information transmission. Axon capacity of transmitting neuronal influx could highly affect one's inhibitory capacities thus creating a more impulsive behavior if not correctly controlled. Since AFD_{fixel} is a novel metric being recently used in tractography studies, to our knowledge, no studies reported associations between AFD_{fixel} and impulsive behaviors in a general pediatric population. However, one study reported a negative association between the fibers density and ADHD symptom severity in ADHD children in some fixels from common WM fascicles such as the corticospinal bundle (Fuelscher et al. 2021). While not entirely comparable, this result converges with the ones reported in the present study.

Impulsivity as multidimensional construct

When considering impulsivity as a complex cognitive function encompassing attentional, motor, and nonplanning impulsiveness, whole-brain FA values have been negatively associated with motor impulsiveness and positively correlated with nonplanning impulsiveness (Goldwaser et al. 2022). In addition, nonplanning impulsiveness were positively correlated with FA values on the superior fronto-occipital fasciculus and motor impulsiveness were negatively correlated with FA values on the corticospinal bundle (Goldwaser et al. 2022). When evaluating connecting regions of these connections, these

results converge with the present study by highlighting connections localized in the frontal, occipital, and parietal regions. On the other hand, results do not fully converge when comparing associations between impulsivity sub-dimensions and WM microstructure. These differences are likely to be due to the complexity of the impulsivity cognitive construct that encompass many other sub-dimensions that our present method is incapable to distinguish. Although reductionist, the use of the CPT-3 as the impulsivity assessment method allows for an objective evaluation as compared with the questionnaire used in this study. Although we reported the same regions, more accuracy in the measurement of these subdimensions would be necessary in order to fully compare our results.

In-connection localization of WM alterations

As a further step in uncovering the relationship between WM microstructure and attentional and impulsive behaviors in a pediatric population, we performed connection profiling of our connections of interest to localize the « altered » regions along each connection. Performing this analysis on all connections allowed us to identified small differences that could be present but not sufficient to drive a significant result in the multivariate analysis. One of the many advantages of connection profiling is the ability to follow the progression of WM microstructure along a specific connection and therefore being able to identify specific regions inside a single connection that presents WM alterations. As mentioned above, dimensionality reduction based on sub-sections metrics yielded slightly different PCs but represented the same biologically interpretable metrics: axonal density and microstructural complexity. Our results showed differences localized closer to the endpoints of connections M6–CD6, A46–LA10, FG37–IOG, and DC–PFT when evaluating both axonal density and microstructural complexity. These endpoints represent the connections with the cortex parcel or the subcortical structure to which each connection is connected. In light of our results, we hypothesize that a difference in either axonal density or microstructural complexity at both or one end of the connection could result in a reduce recruitment capabilities of the functional units localized in the cortex or subcortical structure. Since functional units are recruited to perform a certain cognitive function, it would be logical to expect a reduce recruitment to modify the response capacity of a specific individual. Evidently, this conclusion needs to be taken with precaution, as connections' endpoints can be influencing by multiple factors such as partial volume and fanning of the connections. In addition, M6–CD6, A46–LA10, and FG37–IOG are local association fibers (U-fibers) defined as connecting adjacent gyri (Schmahmann et al. 2008) and are playing a role in brain function (e.g. sensory–motor integration) (Catani et al. 2012; Catani et al. 2017) and in aging and brain development (Phillips et al. 2013; M. Wu et al. 2014a; Nazeri et al. 2015; Wu et al. 2016). Due to methodological challenge, these U-fibers are underrepresented in dMRI studies since high-resolution and specific tractography model such as ours are needed to correctly map these connections (Movahedian Attar et al. 2020), being able to identify these fibers provides new insights in our understanding of attentional skills and impulsive behavior. DC–PFT is part of the thalamic peduncles (Schmahmann et al. 2008) connecting the right dorsal caudate nucleus to the right lateral prefrontal thalamus. An alteration toward the end of the connection can be seen as a reduce innervation in the thalamic nucleus, resulting in a less effective relay center to other regions of the cortex as it is the principal role of the lateral thalamus (Herrero et al. 2002). In addition, this connection is part of the frontal cortex–basal ganglia system that has been reported to be implicated in attention, working memory, and socioemotional behavior (Wise et al. 1996). All these hypotheses converge toward one specific concept: WM alterations reduce the capability of recruiting functional unit in the cortex or in relaying the information toward the cortex.

WM alterations' origins

Although the main goal of this study is to evaluate the relationship between attention/impulsivity and WM microstructure in a population-based children population, one can be wondering how and when these changes happen during the neurodevelopmental trajectories. Multiple factors have been suggested to impact the WM development such as environmental interactions, learning, or intense activities (Fields 2008; Zatorre et al. 2012). While the mechanism underneath these changes are unclear, it has been suggested that activity-dependent myelination could be a strong contributing factor to the differential neurodevelopmental trajectories (Fields 2015). Evidently, uncovering the mechanism underneath these changes would provide a more complete answer to explain the results found in this study. During the 3 decades of neurodevelopmental steps, the human brain goes through many processes such as the myelination of cortical pathways during the late infancy or the overproduction, pruning and stabilization of cortical synapses during the second year of life that have been documented to be essential in cognitive development (Kostović et al. 2019). One review paper by Norbom and colleagues clearly mapped the overall morphological changes that occurs during the development of the more basic and sensory function and also the more high-end cognitive function and how interactions could impact this typical neurodevelopment (Norbom et al. 2021). It is therefore important to consider that the WM alterations reported in this paper could be a result of multiple impacting factors that happened during a child's neurodevelopment.

Summary of findings

Finally, to our knowledge, this is the first study using new state-of-the-art statistical and diffusion approaches

to evaluate attentional skills and impulsive behavior in children from a general population. As a result, we reported the implication of small local associations WM fibers located in the frontal, parietal, basal ganglia, occipital, and temporal regions. We also report an association between higher microstructural complexity or axonal density and a lower impulsive behavior in a general children population. On a within-connection level, we reported implications of WM alterations localized in one or both endpoints of the connection were associated with the variability of attentional skills and impulsive behavior. Evidently, converging studies using these new processing and statistical methods are needed to confirm our hypotheses, but this study brings us closer to a biologically sustained model of attentional skills and impulsive behavior.

Acknowledgements

The authors would like to thank all GESTE participants for their implication and GESTE team members for their hard work in collecting the data.

Funding

This work received funding from the National Institute of Environmental Health Sciences (Grant #R01ES027845) and the « Excellence de Sève » scholarship of the Faculty of Medicine and Health Science at Sherbrooke's University. The funders were not involved in study design, data collection and analysis, preparation of the manuscript and decision to publish.

Conflict of interest statement: M. Descoteaux is CSO and co-founder at Imeka Solutions Inc (www.imeka.ca). C. Bocti holds an investment in Imeka Solutions Inc.

References

Almeida LG, Ricardo-Garcell J, Prado H, Barajas L, Fernández-Bouzas A, Ávila D, Martínez RB. Reduced right frontal cortical thickness in children, adolescents and adults with ADHD and its correlation to clinical variables: a cross-sectional study. *J Psychiatr Res*. 2010:44(16):1214–1223. https://doi.org/10.1016/j.jpsychires.2010.04.026.

Ambrosino S, de Zeeuw P, Wierenga LM, van Dijk S, Durston S. What can cortical development in attention-deficit/hyperactivity disorder teach us about the early developmental mechanisms involved? *Cereb Cortex*. 2017:27(9):4624–4634. https://doi.org/10.1093/cercor/bhx182.

Ameis SH, Lerch JP, Taylor MJ, Lee W, Viviano JD, Pipitone J, Nazeri A, Croarkin PE, Voineskos AN, Lai M-C, et al. A diffusion tensor imaging study in children with ADHD, autism spectrum disorder, OCD, and matched controls: distinct and non-distinct white matter disruption and dimensional brain-behavior relationships. *Am J Psychiatry*. 2016:173(12):1213–1222. https://doi.org/10.1176/appi.ajp.2016.15111435.

Aron AR, Poldrack RA. Cortical and subcortical contributions to stop signal response inhibition: role of the subthalamic nucleus. *J Neurosci*. 2006:26(9):2424–2433. https://doi.org/10.1523/JNEUROSCI.4682-05.2006.

Aron AR, Behrens TE, Smith S, Frank MJ, Poldrack RA. Triangulating a cognitive control network using diffusion-weighted magnetic resonance imaging (MRI) and functional MRI. *J Neurosci*. 2007:27(14):3743–3752. https://doi.org/10.1523/JNEUROSCI.0519-07.2007.

Avants BB, Tustison N, Johnson H. Advanced normalization tools (ants). *Insight J*. 2009;2:1–35.

Bari A, Robbins TW. Inhibition and impulsivity: behavioral and neural basis of response control. *Prog Neurobiol*. 2013:108:44–79. https://doi.org/10.1016/j.pneurobio.2013.06.005.

Basser PJ, Pierpaoli C. Microstructural and physiological features of tissues elucidated by quantitative-diffusion-tensor MRI. *J Magn Reson B*. 1996:111(3):209–219. https://doi.org/10.1006/jmrb.1996.0086.

Biederman J, Petty CR, Woodworth KY, Lomedico A, Hyder LL, Faraone SV. Adult outcome of attention-deficit/hyperactivity disorder: a controlled 16-year follow-up study. *J Clin Psychiatry*. 2012:73(07):941–950. https://doi.org/10.4088/JCP.11m07529.

Cao Q, Shu N, An L, Wang P, Sun L, Xia M-R, Wang J-H, Gong G-L, Zang Y-F, Wang Y-F, et al. Probabilistic diffusion tractography and graph theory analysis reveal abnormal white matter structural connectivity networks in drug-naive boys with attention deficit/hyperactivity disorder. *J Neurosci*. 2013:33(26):10676–10687.

Catani M, Dell'Acqua F, Vergani F, Malik F, Hodge H, Roy P, Valabregue R, Thiebaut de Schotten M. Short frontal lobe connections of the human brain. *Cortex*. 2012:48(2):273–291. https://doi.org/10.1016/j.cortex.2011.12.001.

Catani M, Robertsson N, Beyh A, Huynh V, de Santiago Requejo F, Howells H, Barrett RLC, Aiello M, Cavaliere C, Dyrby TB, et al. Short parietal lobe connections of the human and monkey brain. *Cortex*. 2017:97:339–357. https://doi.org/10.1016/j.cortex.2017.10.022.

Cha J, Fekete T, Siciliano F, Biezonski D, Greenhill L, Pliszka SR, Blader JC, Krain Roy A, Leibenluft E, Posner J. Neural correlates of aggression in medication-naive children with ADHD: multivariate analysis of morphometry and tractography. *Neuropsychopharmacology*. 2015:40(7):1717–1725. https://doi.org/10.1038/npp.2015.18.

Chamberland M, Raven EP, Genc S, Duffy K, Descoteaux M, Parker GD, Tax CMW, Jones DK. Dimensionality reduction of diffusion MRI measures for improved tractometry of the human brain. *NeuroImage*. 2019:200:89–100. https://doi.org/10.1016/j.neuroimage.2019.06.020.

Chevrier AD, Noseworthy MD, Schachar R. Dissociation of response inhibition and performance monitoring in the stop signal task using event-related fMRI. *Hum Brain Mapp*. 2007:28(12):1347–1358. https://doi.org/10.1002/hbm.20355.

Cortese S, Kelly C, Chabernaud C, Proal E, Di Martino A, Milham MP, Castellanos FX. Toward systems neuroscience of ADHD: a meta-analysis of 55 fMRI studies. *AJP*. 2012:169(10):1038–1055. https://doi.org/10.1176/appi.ajp.2012.11101521.

Cousineau M, Jodoin P-M, Garyfallidis E, Côté M-A, Morency FC, Rozanski V, Grand'Maison M, Bedell BJ, Descoteaux M. A test-retest study on Parkinson's PPMI dataset yields statistically significant white matter fascicles. *NeuroImage: Clinical*. 2017:16:222–233. https://doi.org/10.1016/j.nicl.2017.07.020.

Descoteaux M, Angelino E, Fitzgibbons S, Deriche R. Regularized, fast, and robust analytical Q-ball imaging. *Magn Reson Med*. 2007:58(3):497–510. https://doi.org/10.1002/mrm.21277.

Descoteaux M, Deriche R, Knosche TR, Anwander A. Deterministic and probabilistic tractography based on complex fibre orientation distributions. *IEEE Trans Med Imaging*. 2009:28(2):269–286. https://doi.org/10.1109/TMI.2008.2004424.

Di Tommaso P, Chatzou M, Floden EW, Barja PP, Palumbo E, Notredame C. Nextflow enables reproducible computational workflows. *Nat Biotechnol*. 2017:35(4):316–319. https://doi.org/10.1038/nbt.3820.

Ellison-Wright I, Ellison-Wright Z, Bullmore E. Structural brain change in attention deficit hyperactivity disorder identified by meta-analysis. *BMC Psychiatry*. 2008:8(1):51. https://doi.org/10.1186/1471-244X-8-51.

Epstein JN, Erkanli A, Conners CK, Klaric J, Costello JE, Angold A. Relations between continuous performance test performance measures and ADHD behaviors. *J Abnorm Child Psychol*. 2003:31(5):543–554. https://doi.org/10.1023/a:1025405216339.

Fan L, Li H, Zhuo J, Zhang Y, Wang J, Chen L, Yang Z, Chu C, Xie S, Laird AR, et al. The Human Brainnetome atlas: a new brain atlas based on connectional architecture. *Cereb Cortex*. 2016:26(8):3508–3526. https://doi.org/10.1093/cercor/bhw157.

Fields RD. White matter in learning, cognition and psychiatric disorders. *Trends Neurosci*. 2008:31(7):361–370. https://doi.org/10.1016/j.tins.2008.04.001.

Fields RD. A new mechanism of nervous system plasticity: activity-dependent myelination. *Nat Rev Neurosci*. 2015:16(12):756–767. https://doi.org/10.1038/nrn4023.

Fischl B. FreeSurfer. *NeuroImage*. 2012:62(2):774–781. https://doi.org/10.1016/j.neuroimage.2012.01.021.

Frodl T, Skokauskas N. Meta-analysis of structural MRI studies in children and adults with attention deficit hyperactivity disorder indicates treatment effects: meta-analysis of structural MRI ADHD studies. *Acta Psychiatr Scand*. 2012:125(2):114–126. https://doi.org/10.1111/j.1600-0447.2011.01786.x.

Fuelscher I, Hyde C, Anderson V, Silk TJ. White matter tract signatures of fiber density and morphology in ADHD. *Cortex*. 2021:138:329–340. https://doi.org/10.1016/j.cortex.2021.02.015.

Garyfallidis E, Brett M, Amirbekian B, Rokem A, van der Walt S, Descoteaux M, Nimmo-Smith I, Contributors D. Dipy, a library for the analysis of diffusion MRI data. *Front Neuroinform*. 2014:8. https://doi.org/10.3389/fninf.2014.00008. [accessed 2021 Jun 28].

Geeraert BL, Chamberland M, Lebel RM, Lebel C. Multimodal principal component analysis to identify major features of white matter structure and links to reading, Yap P-T, editor. *PLoS One*. 2020:15(8):e0233244. https://doi.org/10.1371/journal.pone.0233244.

Goldwaser EL, Du X, Adhikari BM, Kvarta M, Chiappelli J, Hare S, Marshall W, Savransky A, Carino K, Bruce H, et al. Role of white matter microstructure in impulsive behavior. *J Neuropsychiatry Clin Neurosci*. 2022. https://doi.org/10.1176/appi.neuropsych.21070167.

Goodale MA, Milner AD. Separate visual pathways for perception and action. *Trends Neurosci*. 1992:15(1):20–25. https://doi.org/10.1016/0166-2236(92)90344-8.

Greven CU, Bralten J, Mennes M, O'Dwyer L, van Hulzen KJE, Rommelse N, Schweren LJS, Hoekstra PJ, Hartman CA, Heslenfeld D, et al. Developmentally stable whole-brain volume reductions and developmentally sensitive caudate and putamen volume alterations in those with attention-deficit/hyperactivity disorder and their unaffected siblings. *JAMA Psychiatry*. 2015:72(5):490. https://doi.org/10.1001/jamapsychiatry.2014.3162.

Guberman GI, Stojanovski S, Nishat E, Ptito A, Bzdok D, Wheeler A, Descoteaux M. Multi-tract multi-symptom relationships in pediatric concussion. *Neurology*. 2021. http://medrxiv.org/lookup/doi/10.1101/2021.04.01.21254814 [accessed 2022 Jan 11].

Hart H, Radua J, Nakao T, Mataix-Cols D, Rubia K. Meta-analysis of functional magnetic resonance imaging studies of inhibition and attention in attention-deficit/hyperactivity disorder: exploring task-specific, stimulant medication, and age effects. *JAMA Psychiatry*. 2013:70(2):185. https://doi.org/10.1001/jamapsychiatry.2013.277.

Herrero M-T, Barcia C, Navarro J. Functional anatomy of thalamus and basal ganglia. *Childs Nerv Syst*. 2002:18(8):386–404. https://doi.org/10.1007/s00381-002-0604-1.

Hong S-B, Zalesky A, Fornito A, Park S, Yang Y-H, Park M-H, Song I-C, Sohn C-H, Shin M-S, Kim B-N, et al. Connectomic disturbances in attention-deficit/hyperactivity disorder: a whole-brain tractography analysis. *Biol Psychiatry*. 2014:76(8):656–663. https://doi.org/10.1016/j.biopsych.2013.12.013.

Hoogman M, Bralten J, Hibar DP, Mennes M, Zwiers MP, Schweren LSJ, van Hulzen KJE, Medland SE, Shumskaya E, Jahanshad N, et al. Subcortical brain volume differences in participants with attention deficit hyperactivity disorder in children and adults: a cross-sectional mega-analysis. *Lancet Psychiatry*. 2017:4(4):310–319. https://doi.org/10.1016/S2215-0366(17)30049-4.

Hutchinson AD, Mathias JL, Banich MT. Corpus callosum morphology in children and adolescents with attention deficit hyperactivity disorder: a meta-analytic review. *Neuropsychology*. 2008:22(3):341–349. https://doi.org/10.1037/0894-4105.22.3.341.

Jenkinson M, Beckmann CF, Behrens TEJ, Woolrich MW, Smith SM. FSL. *NeuroImage*. 2012:62(2):782–790. https://doi.org/10.1016/j.neuroimage.2011.09.015.

Jeurissen B, Leemans A, Tournier J-D, Jones DK, Sijbers J. Investigating the prevalence of complex fiber configurations in white matter tissue with diffusion magnetic resonance imaging: prevalence of multifiber voxels in WM. *Hum Brain Mapp*. 2013:34(11):2747–2766. https://doi.org/10.1002/hbm.22099.

Jones DK. Challenges and limitations of quantifying brain connectivity *in vivo* with diffusion MRI. *Imaging Med*. 2010:2(3):341–355. https://doi.org/10.2217/iim.10.21.

Jones DK, Knösche TR, Turner R. White matter integrity, fiber count, and other fallacies: the do's and don'ts of diffusion MRI. *NeuroImage*. 2013:73:239–254. https://doi.org/10.1016/j.neuroimage.2012.06.081.

Kostović I, Sedmak G, Judaš M. Neural histology and neurogenesis of the human fetal and infant brain. *NeuroImage*. 2019:188:743–773. https://doi.org/10.1016/j.neuroimage.2018.12.043.

Kurtzer GM, Sochat V, Bauer MW. Singularity: scientific containers for mobility of compute, Gursoy A, editor. *PLoS One*. 2017:12(5):e0177459. https://doi.org/10.1371/journal.pone.0177459.

Lei D, Du M, Wu M, Chen T, Huang X, Du X, Bi F, Kemp GJ, Gong Q. Functional MRI reveals different response inhibition between adults and children with ADHD. *Neuropsychology*. 2015:29(6):874–881. https://doi.org/10.1037/neu0000200.

Lin Q, Bu X, Wang M, Liang Y, Chen H, Wang W, Yi Y, Lin H, Zhou J, Lu L, et al. Aberrant white matter properties of the callosal tracts implicated in girls with attention-deficit/hyperactivity disorder. *Brain Imaging Behav*. 2020:14(3):728–735. https://doi.org/10.1007/s11682-018-0010-2.

Madsen KS, Baaré WFC, Vestergaard M, Skimminge A, Ejersbo LR, Ramsøy TZ, Gerlach C, Åkeson P, Paulson OB, Jernigan TL. Response inhibition is associated with white matter microstructure in children. *Neuropsychologia*. 2010:48(4):854–862. https://doi.org/10.1016/j.neuropsychologia.2009.11.001.

Mayorga-Weber G, Rivera FJ, Castro MA. Neuron-glia (mis)interactions in brain energy metabolism during aging. *J Neurosci Res*. 2022. https://doi.org/10.1002/jnr.25015.

McCarthy H, Skokauskas N, Frodl T. Identifying a consistent pattern of neural function in attention deficit hyperactivity disorder: a meta-analysis. *Psychol Med*. 2014:44(4):869–880. https://doi.org/10.1017/S0033291713001037.

Mischel W, Ebbesen EB. Attention in delay of gratification. *J Pers Soc Psychol*. 1970:16(2):329–337. https://doi.org/10.1037/h0029815.

Movahedian Attar F, Kirilina E, Haenelt D, Pine KJ, Trampel R, Edwards LJ, Weiskopf N. Mapping short association fibers in the early cortical visual processing stream using in vivo diffusion tractography. *Cereb Cortex*. 2020:30(8):4496–4514. https://doi.org/10.1093/cercor/bhaa049.

Nakao T, Radua J, Rubia K, Mataix-Cols D. Gray matter volume abnormalities in ADHD: voxel-based meta-analysis exploring the effects of age and stimulant medication. *Am J Psychiatry*. 2011:168(11):1154–1163. https://doi.org/10.1176/appi.ajp.2011.11020281.

Narr KL, Woods RP, Lin J, Kim J, Phillips OR, Del'Homme M, Caplan R, Toga AW, McCracken JT, Levitt JG. Widespread cortical thinning is a robust anatomical marker for attention-deficit/hyperactivity disorder. *J Am Acad Child Adolesc Psychiatry*. 2009:48(10):1014–1022. https://doi.org/10.1097/CHI.0b013e3181b395c0.

Nazeri A, Chakravarty MM, Rajji TK, Felsky D, Rotenberg DJ, Mason M, Xu LN, Lobaugh NJ, Mulsant BH, Voineskos AN. Superficial white matter as a novel substrate of age-related cognitive decline. *Neurobiol Aging*. 2015:36(6):2094–2106. https://doi.org/10.1016/j.neurobiolaging.2015.02.022.

Norbom LB, Ferschmann L, Parker N, Agartz I, Andreassen OA, Paus T, Westlye LT, Tamnes CK. New insights into the dynamic development of the cerebral cortex in childhood and adolescence: integrating macro- and microstructural MRI findings. *Prog Neurobiol*. 2021:204:102109. https://doi.org/10.1016/j.pneurobio.2021.102109.

Norman LJ, Carlisi C, Lukito S, Hart H, Mataix-Cols D, Radua J, Rubia K. Structural and functional brain abnormalities in attention-deficit/hyperactivity disorder and obsessive-compulsive disorder: a comparative meta-analysis. *JAMA Psychiatry*. 2016:73(8):815. https://doi.org/10.1001/jamapsychiatry.2016.0700.

Ord AS, Miskey HM, Lad S, Richter B, Nagy K, Shura RD. Examining embedded validity indicators in Conners continuous performance test-3 (CPT-3). *Clin Neuropsychol*. 2021:35(8):1426–1441. https://doi.org/10.1080/13854046.2020.1751301.

Pedregosa F, Varoquaux G, Gramfort A, Michel V, Thirion B, Grisel O, Blondel M, Prettenhofer P, Weiss R, Dubourg V, et al. Scikit-learn: machine Learning in Python. *J Mach Learn Res*. 2011:12:6.

Phillips OR, Clark KA, Luders E, Azhir R, Joshi SH, Woods RP, Mazziotta JC, Toga AW, Narr KL. Superficial white matter: effects of age, sex, and hemisphere. *Brain Connectivity*. 2013:3(2):146–159. https://doi.org/10.1089/brain.2012.0111.

Polanczyk GV, Salum GA, Sugaya LS, Caye A, Rohde LA. Annual research review: a meta-analysis of the worldwide prevalence of mental disorders in children and adolescents. *J Child Psychol Psychiatry*. 2015:56(3):345–365. https://doi.org/10.1111/jcpp.12381.

Posner J, Polanczyk GV, Sonuga-Barke E. Attention-deficit hyperactivity disorder. *Lancet*. 2020:395(10222):450–462. https://doi.org/10.1016/S0140-6736(19)33004-1.

Puiu AA, Wudarczyk O, Goerlich KS, Votinov M, Herpertz-Dahlmann B, Turetsky B, Konrad K. Impulsive aggression and response inhibition in attention-deficit/hyperactivity disorder and disruptive behavioral disorders: findings from a systematic review. *Neurosci Biobehav Rev*. 2018:90:231–246. https://doi.org/10.1016/j.neubiorev.2018.04.016.

Qiu A, Rifkin-Graboi A, Tuan TA, Zhong J, Meaney MJ. Inattention and hyperactivity predict alterations in specific neural circuits among 6-year-old boys. *J Am Acad Child Adolesc Psychiatry*. 2012:51(6):632–641.

Raffelt DA, Tournier J-D, Smith RE, Vaughan DN, Jackson G, Ridgway GR, Connelly A. Investigating white matter fibre density and morphology using fixel-based analysis. *NeuroImage*. 2017:144:58–73. https://doi.org/10.1016/j.neuroimage.2016.09.029.

Rubia K, Smith AB, Brammer MJ, Taylor E. Right inferior prefrontal cortex mediates response inhibition while mesial prefrontal cortex is responsible for error detection. *NeuroImage*. 2003:20(1):351–358. https://doi.org/10.1016/S1053-8119(03)00275-1.

Rubia K, Alegria A, Brinson H. Imaging the ADHD brain: disorder-specificity, medication effects and clinical translation. *Expert Rev Neurother*. 2014:14(5):519–538. https://doi.org/10.1586/14737175.2014.907526.

Schmahmann JD, Smith EE, Eichler FS, Filley CM. Cerebral white matter. *Ann N Y Acad Sci*. 2008:1142(1):266–309. https://doi.org/10.1196/annals.1444.017.

Scimeca LM, Holbrook L, Rhoads T, Cerny BM, Jennette KJ, Resch ZJ, Obolsky MA, Ovsiew GP, Soble JR. Examining Conners continuous performance test-3 (CPT-3) embedded performance validity indicators in an adult clinical sample referred for ADHD evaluation. *Dev Neuropsychol*. 2021:46(5):347–359. https://doi.org/10.1080/87565641.2021.1951270.

Seabold S, Perktold J. 2010. *Statsmodels: econometric and statistical modeling with Python*. Austin, Texas. p. 92–96. [accessed 2021 Nov 9]. https://conference.scipy.org/proceedings/scipy2010/seabold.html.

Seehaus A, Roebroeck A, Bastiani M, Fonseca L, Bratzke H, Lori N, Vilanova A, Goebel R, Galuske R. Histological validation of high-resolution DTI in human post mortem tissue. *Front Neuroanat*. 2015:9. https://doi.org/10.3389/fnana.2015.00098 . [accessed 2021 Apr 13].

Shaw P, Eckstrand K, Sharp W, Blumenthal J, Lerch JP, Greenstein D, Clasen L, Evans A, Giedd J, Rapoport JL. Attention-deficit/hyperactivity disorder is characterized by a delay in cortical maturation. *Proc Natl Acad Sci*. 2007:104(49):19649–19654. https://doi.org/10.1073/pnas.0707741104.

Shaw P, Malek M, Watson B, Sharp W, Evans A, Greenstein D. Development of cortical surface area and gyrification in attention-deficit/hyperactivity disorder. *Biol Psychiatry*. 2012:72(3):191–197. https://doi.org/10.1016/j.biopsych.2012.01.031.

Sherif T, Rioux P, Rousseau M-E, Kassis N, Beck N, Adalat R, Das S, Glatard T, Evans AC. CBRAIN: a web-based, distributed computing platform for collaborative neuroimaging research. *Front Neuroinform*. 2014:8. https://doi.org/10.3389/fninf.2014.00054. [accessed 2021 Nov 8].

Shoda Y, Mischel W, Peake PK. Predicting adolescent cognitive and self-regulatory competencies from preschool delay of gratification: identifying diagnostic conditions. Developmental Psychology, 1990;26(6):978–986. https://doi.org/10.1037/0012-1649.26.6.978.

Silk TJ, Genc S, Anderson V, Efron D, Hazell P, Nicholson JM, Kean M, Malpas CB, Sciberras E. Developmental brain trajectories in children with ADHD and controls: a longitudinal neuroimaging study. *BMC Psychiatry*. 2016:16(1):59. https://doi.org/10.1186/s12888-016-0770-4.

Smith M. 2021. Chapter 3 - brain mapping. In: Smith M, editor. *Mechanisms and genetics of neurodevelopmental cognitive disorders*. Academic Press. p. 49–76. https://www.sciencedirect.com/science/article/pii/B9780128219133000044.

Sonuga-Barke EJS, Castellanos FX. Spontaneous attentional fluctuations in impaired states and pathological conditions: a neurobiological hypothesis. *Neurosci Biobehav Rev*. 2007:31(7):977–986. https://doi.org/10.1016/j.neubiorev.2007.02.005.

Sudre G, Bouyssi-Kobar M, Norman L, Sharp W, Choudhury S, Shaw P. Estimating the heritability of developmental change in neural connectivity, and its association with changing symptoms of attention-deficit/hyperactivity disorder. *Biol Psychiatry*. 2020. https://doi.org/10.1016/j.biopsych.2020.06.007.

Theaud G, Houde J-C, Boré A, Rheault F, Morency F, Descoteaux M. TractoFlow: a robust, efficient and reproducible diffusion MRI pipeline leveraging Nextflow & singularity. *NeuroImage*. 2020:218:116889. https://doi.org/10.1016/j.neuroimage.2020.116889.

Tournier J-D, Calamante F, Connelly A. Robust determination of the fibre orientation distribution in diffusion MRI: non-negativity constrained super-resolved spherical deconvolution. *NeuroImage*. 2007:35(4):1459–1472. https://doi.org/10.1016/j.neuroimage.2007.02.016.

Tournier J-D, Smith R, Raffelt D, Tabbara R, Dhollander T, Pietsch M, Christiaens D, Jeurissen B, Yeh C-H, Connelly A. MRtrix3: a fast, flexible and open software framework for medical image processing and visualisation. *NeuroImage*. 2019:202:116137. https://doi.org/10.1016/j.neuroimage.2019.116137.

Valera EM, Faraone SV, Murray KE, Seidman LJ. Meta-analysis of structural imaging findings in attention-deficit/hyperactivity disorder. *Biol Psychiatry*. 2007:61(12):1361–1369. https://doi.org/10.1016/j.biopsych.2006.06.011.

Wise SP, Murray EA, Gerfen CR. The frontal cortex-basal ganglia system in primates. *Crit Rev Neurobiol*. 1996:10(3–4):317–356. https://doi.org/10.1615/critrevneurobiol.v10.i3-4.30.

Wu M, Kumar A, Yang S. Development and aging of superficial white matter myelin from young adulthood to old age: mapping by vertex-based surface statistics (VBSS). *Hum Brain Mapp*. 2016:37(5):1759–1769. https://doi.org/10.1002/hbm.23134.

Wu M, Lu LH, Lowes A, Yang S, Passarotti AM, Zhou XJ, Pavuluri MN. Development of superficial white matter and its structural interplay with cortical gray matter in children and adolescents: development of SWM in children and adolescents. *Hum Brain Mapp*. 2014a:35(6):2806–2816. https://doi.org/10.1002/hbm.22368.

Wu Y-H, Gau SS-F, Lo Y-C, Tseng W-YI. White matter tract integrity of frontostriatal circuit in attention deficit hyperactivity disorder: association with attention performance and symptoms. *Hum Brain Mapp*. 2014b:35(1):199–212.

Yeatman JD, Dougherty RF, Myall NJ, Wandell BA, Feldman HM. Tract profiles of white matter properties: automating fiber-tract quantification, Beaulieu C, editor. *PLoS One*. 2012:7(11):e49790. https://doi.org/10.1371/journal.pone.0049790.

Zatorre RJ, Fields RD, Johansen-Berg H. Plasticity in gray and white: neuroimaging changes in brain structure during learning. *Nat Neurosci*. 2012:15(4):528–536. https://doi.org/10.1038/nn.3045.

Zhan C, Liu Y, Wu K, Gao Y, Li X. Structural and functional abnormalities in children with attention-deficit/hyperactivity disorder: a focus on subgenual anterior cingulate cortex. *Brain Connect*. 2017:7(2):106–114. https://doi.org/10.1089/brain.2016.0444.